Human and mouse Gpi1p homologues restore glycosylphosphatidylinositol membrane anchor biosynthesis in yeast mutants

Andreas TIEDE*, Jörg SCHUBERT*, Claudia NISCHAN*, Irene JENSEN†, Barbara WESTFALL†, Christopher H. TARON†, Peter ORLEAN† and Reinhold E. SCHMIDT*[1]

*Department of Clinical Immunology, Hannover Medical School, Carl-Neuberg-Str. 1, D-30625 Hannover, Germany, and †Department of Biochemistry, University of Illinois, Urbana, IL 61801, U.S.A.

Glycosylphosphatidylinositol (GPI) represents an important anchoring molecule for cell surface proteins. The first step in its synthesis is the transfer of *N*-acetylglucosamine (GlcNAc) from UDP to phosphatidylinositol (PI). The products of three mammalian genes, *PIG-A*, *PIG-C* and *PIG-H*, have previously been shown to be involved in the putative enzymic complex. Here we report the cloning of human and mouse cDNAs encoding a fourth participant in the GlcNAc transfer reaction which are homologues of the *Saccharomyces cerevisiae* and *Schizosaccharomyces pombe* Gpi1 proteins. To provide evidence for their function, these proteins were expressed in *GPI1*-disrupted yeast strains. In *Sacch. cerevisiae*, where *GPI1* disruption results in a temperature-sensitive phenotype and abolishes *in vitro* GlcNAc-PI synthesis, restoration of growth could be demonstrated in a temperature-dependent manner. In addition, *in vitro* GlcNAc-PI synthetic activity was again detectable. In *Schiz. pombe*, *gpi1*$^+$ disruption is lethal. Using random spore analysis, we were able to show that the mammalian *GPI1* homologues can rescue haploids harbouring the lethal *gpi1*$^+$::*his7*$^+$ allele. Our data demonstrate that the genes identified are indeed involved in the first step of GPI biosynthesis, and allow conclusions about a specific function for Gpi1p in stabilizing the enzymic complex. The finding that, despite a low degree of identity, the mammalian Gpi1 proteins are able to participate in the yeast GlcNAc-PI synthetic machinery as heterologous components further demonstrates that GPI biosynthesis has been highly conserved throughout evolution.

INTRODUCTION

Many cell surface proteins in eukaryotes are attached to the cell membrane through the hydrocarbon chains of a covalently bound glycosylphosphatidylinositol (GPI) membrane anchor, rather than by a classical transmembrane domain [1]. Anchoring by GPI can dramatically alter the functional properties of a protein, as shown for instance for human immunoglobulin receptors that exist in both GPI-anchored and transmembrane forms [2]. Pathophysiological studies of paroxysmal nocturnal haemoglobinuria (PNH), a bone marrow disorder caused by a deficiency in GPI biosynthesis [3–5], have demonstrated the great importance of GPI anchoring for regulation of cell growth and activation [6,7]. In eukaryotic microbes, GPIs are important for growth and morphogenesis [8]. Mutations in GPI biosynthetic genes in *Saccharomyces cerevisiae* and *Schizosaccharomyces pombe* lead to conditional lethality and defects in cell division [9,10]. Therefore GPI biosynthesis could be exploited as a possible target for future selective anti-microbial agents.

The biosynthesis of GPI anchors takes place in the endoplasmic reticulum [11]. The first step is the transfer of *N*-acetylglucosamine (GlcNAc) from UDP to phosphatidylinositol (PI). This step is of special interest, as it is affected in PNH and could also be the committed step for regulation of GPI biosynthesis that seems to play a role in cell activation [6]. Analysis of GPI-anchoring-defective mammalian and yeast cell lines [9,12] has revealed the genetic requirements for this biochemical reaction to be unexpectedly complex. Three mammalian genes, *PIG-A* [13], *PIG-C* [14] and *PIG-H* [15], as well as three *Sacch. cerevisiae* genes, *GPI1* [16], *GPI2* [17] and *GPI3*/*SPT14*/*CWH6* [17–20], have been shown to be involved. Sequence comparisons demonstrated that *GPI3* and *GPI2* encode homologues of the Pig-a and Pig-c proteins respectively, but no obvious similarity was found between the Gpi1 and Pig-h proteins. This led to speculation about the existence of a fourth participant in the GlcNAc transfer reaction, i.e. a mammalian homologue of the yeast *GPI1* gene, as well as a yeast counterpart of *PIG-H*. However, throughout the *Sacch. cerevisiae* genome no open reading frame (ORF) with significant identity with *PIG-H* was detectable using conventional sequence comparison software. In addition, among the numerous GPI-deficient mammalian cell lines analysed in different laboratories, only cells of mutation classes A, C and H are blocked in the first step of the biosynthetic pathway. Therefore the lack of similarity between *GPI1* and *PIG-H* could be interpreted as evolutionary development rather than being indicative of the existence of a further component in the enzymic complex.

In order to confirm one of these contrasting hypotheses, we searched for a mammalian homologue of yeast Gpi1p. After identification of human and mouse genes encoding putative homologues, these were expressed in Δ*gpi1* mutant *Sacch. cerevisiae* and *Schiz. pombe* strains. In *Sacch. cerevisiae*, *GPI1* disruption results in an inability to grow at temperatures higher than 25 °C [16], whereas *gpi1*$^+$ disruption in *Schiz. pombe* is lethal

Abbreviations used: EST expressed sequence tag; GlcNAc-PI, *N*-acetylglucosaminylphosphatidylinositol; GlcN-PI, glucosaminylphosphatidylinositol; GPI, glycosylphosphatidylinositol; ORF, open reading frame; PI, phosphatidylinositol; PI-PLC, PI-specific phospholipase C; PNH, paroxysmal nocturnal haemoglobinuria; RACE, rapid amplification of cDNA ends; the prefixes Sc, Hs and Mm denote *Saccharomyces cerevisiae*, human (*Homo sapiens*) and mouse (*Mus musculus*) genes/proteins respectively.

[1] To whom correspondence should be addressed (e-mail immunologie@mh-hannover.de).

The nucleotide sequences of the human and mouse *GPI1* genes have been deposited in the GenBank, EMBL and DDBJ Nucleotide Sequence Databases under accession numbers AF030177 and AF030178 respectively.

[10]. Partial complementation of these mutant phenotypes provided strong evidence that the newly identified genes are indeed functional homologues of the yeast *GPI1* genes. The fact that these gene products are able to participate in the yeast GlcNAc synthetic machinery demonstrates the high degree of evolutionary conservation in the structure of the enzymic complex.

MATERIALS AND METHODS

Yeast strains and culture media

The *Sacch. cerevisiae gpi1*-disrupted strain was created by replacing one of the *GPI1* genes in diploid strain YMW3 [21] with the *TRP1* selectable marker, as described in Fig. 3B in [16]. This diploid was then sporulated and the haploid meiotic segregant *gpi1*::*TRP1 ade2-1 ade3D22 his3-11,15 leu2-3,112 trp1-1 ura3-1 can1-100* was isolated. Cells were cultured on standard solid and liquid YPD or YNB media [22]. The *Schiz. pombe gpi1*$^+$ heterozygous diploid strain (*gpi1*$^+$/*gpi1*$^+$::*his7*$^+$ *ade6-M210*/*ade6-M216 leu1-32*/*leu1-32 ura4-d18*/*ura4-d18*) was described previously [10]. *Schiz. pombe* cells were grown in supplemented synthetic EMM2 medium at 30 °C [23].

Database searching

The *tblastn* algorithm was used to search the EST (expressed sequence tag) database for cDNA clones encoding proteins similar to *Sacch. cerevisiae* Gpi1p (ScGpi1p) [24,25]. Three 5′ ESTs (T97832, F07500 and R24980) showed significant identity with C-terminal amino acids of Gpi1p, indicating that these were only partial clones. To identify longer clones, the EST database was searched with the 3′ ESTs corresponding to the identified 5′ sequences (T97729, Z40563 and R45240) using the *blastn* program. Seven human clones were found. Among these, the longest clone (30904; accession no. for 3′ EST: R41932) had an insert of approx. 2.5 kb, although it was reported to contain 2.965 kb by the I.M.A.G.E. consortium [26]. This clone was provided by the Resource Center/Primary Database of the German Human Genome Project and sequenced. Later in the process of verifying the cDNA sequence of *HsGPI1* [where Hs denotes human (*Homo sapiens*)], clone 30904 was found to contain an unspliced intron of 164 bp (between nucleotides 892 and 893 in the final sequence reported). Murine *GPI1* (EST clone 404783 from C57BL/6J adult brain; accession no. for 5′ EST: AA072344) was identified by searching the EST database with the *blastn* program and the final sequence of *HsGPI1*.

DNA synthesis and sequence analysis

DNA oligomer synthesis was carried out by MWG Biotech (Ebersberg, Germany) and the Genetic Engineering Facility of the University of Illinois, Urbana. DNA sequencing was performed by Eric C. Böttger and co-workers (Hannover Medical School, Germany) and MWG Biotech. For DNA and protein sequence analysis we used PCGene (IntelliGenetics Inc.), DNA Strider 1.1 [27], CLUSTAL W 1.06 [28], MACAW [29], the PROSITE package [30] and PHDtopology [31].

Northern hybridization

Either 5 or 20 μg of total RNA from HL-60 cells and a ^{32}P-labelled probe from the insert of clone 30904 were used for Northern blot analysis. Filters were hybridized in ExpressHyb solution (Clontech) following the manufacturer's instructions and washed for 3×30 min in $5\times$, $1\times$ and $0.2\times$ SSC at 68 °C.

Cloning of the 5′ end of *HsGPI1* by a RACE (rapid amplification of cDNA ends) PCR-related technique

Marathon Ready cDNA from human bone marrow was obtained from Clontech Inc. PCR was carried out with a gene-specific primer GSP (5′-ATAGGATCCACGTCCAGCAGCACAGAGGCCACCGTGTTGGCC), which contains a *Bam*HI site (underlined), and the AP1 anchor primer provided by the manufacturer under the following conditions: 5 cycles (30 s at 95 °C; 2 min at 72 °C); 5 cycles (30 s at 95 °C; 2 min at 68 °C); 20 cycles (30 s at 95 °C; 2 min at 60 °C). PCR products were cloned into the pBlueScript SK$^+$ vector (Stratagene) using a *Not*I site on AP1 and the *Bam*HI site engineered into the GSP primer. The complete coding region of *HsGPI*1 was amplified by reverse transcription–PCR with avian myeloblastosis virus reverse transcriptase (Promega) and Vent polymerase (New England Biolabs) out of HL-60 RNA using primer Rev (5′-GTGTTCAGGAGCACAC) for first-strand synthesis and primers U-Hs (5′-ATTGGATCCCATCGGGGTCCCCAACCCCATCCGGACC; *Bam*HI site underlined) and D-Hs (5′-ATAGGTACCTCAGTCCTGCTTGTCCCCTCTCTGC; *Kpn*I site underlined) for PCR.

Construction of *Sacch. cerevisiae* expression plasmids

Coding regions of mammalian *GPI1* genes were cloned directly behind the *ScGPI1* promoter by fusing overlapping PCR products of the promoter and the gene of interest. First, the *ScGPI1* promoter was PCR-amplified with primers U-Sc (5′-ATTGGATCCGTGGTTTTGATTCTAGACGGTTACC; *Bam*HI site underlined) and F4 [5′-GGGGAAGAAGGCCTTGAGCACCATGTCATTTAACTGTATAAACCGCCC; the 5′ half underlined is complementary to the start of the *HsGPI1* and *MmGPI1* ORF, where Mm denotes mouse (*Mus musculus*)] using Vent polymerase. Secondly, the *HsGPI1* and *MmGPI1* ORFs were amplified with primer F3 (5′-GGGCGGTTTATACAGTTAAATGACATGGTGCTCAAGGCCTTCTTCCCC; the 5′ half underlined is identical to the end of the *ScGPI1* promoter) and D-Hs (see above; since the mouse and human nucleotide sequences are almost identical at the primer binding sites, the same primers were used in both PCRs). Thirdly, the partially complementary fragments were fused in five PCR cycles without primers, and fusion products were subsequently amplified in another 15 PCR cycles with primers U-Sc and D-Hs. Using an analogous approach, a yeast–human chimaeric ORF was constructed with primers F1 (5′-GGCTTATTATTAATGACATTTCATTTGGTTTAATGCTGCTGTCCTGGCTCCACGGGAGAAGCGC) and F2 (5′-GCGCTTCTCCCGTGGAGCCAGGACAGCAGCATTAAACCAAATGAAATGTCATTAATAATAAGCC) instead of F3 and F4 respectively. In the resulting chimaera, ScGpi1p amino acids 302–609 are replaced by HsGpi1p amino acids 289–581. Using *Bam*HI and *Kpn*I restriction sites, PCR products were cloned into the *URA3*-selectable vectors pRS416 and pRS426 (Stratagene), containing the CEN and 2μ origins of replication respectively. For negative controls, pRS416 was used alone. For positive controls, *ScGPI1* was cloned into pRS416.

Construction of *Schiz. pombe* expression plasmids

The coding regions of *HsGPI*1 and *MmGPI*1 were PCR-amplified with primers U-Hs-*Nde*I [5′-ATTCATATGGTGCTCAAGGCCTTCTTCCCCACG; upstream AUG context is mutated into an *Nde*I restriction site (underlined)] and D-Hs-*Bam*HI (5′-ATAGGATCCTCAGTCCTGCTTGTCCCCTCTCTGC; *Bam*HI site underlined). Using the introduced *Nde*I and *Bam*HI

restriction sites, PCR products were cloned directly behind the *nmt1* thiamin-repressible promoter of the *leu-32*-selectable pREP1 vector [32]. For negative controls, pREP1 was used alone. For positive controls, a plasmid containing *Schiz. pombe* *gpi1*$^+$ was used (pPVSG1; described in [10]).

Complementation of temperature-sensitivity in *Sacch. cerevisiae*

Plasmid transformation was carried out using the standard lithium acetate procedure [22]. At least 10 independent recombinant clones from each transformation were tested for correction of temperature-sensitivity by incubating plates for 6 days at the indicated temperature immediately after re-streaking.

Enzyme assays

The *in vitro* synthesis of ^{14}C-labelled GPI precursors was assayed in twice-washed mixed membranes freshly prepared as described previously [33] from transformants grown to $A_{600} = 1.0$ in minimal medium at 25 °C. Lipids were extracted in chloroform/methanol (3:2, v/v) and washed twice with Folch theoretical upper phase (49 % methanol, 48 % water, 3 % chloroform, 4 μM $MgCl_2$). Chemical and enzymic characterization was accomplished as described in [33]. Lipids were then separated by TLC on Kieselgel 60 sheets (Merck) using chloroform/methanol/water (65:25:4, by vol.) as solvent and visualized either using a Tracemaster 20 linear scanner (Chroma 2D, Berthold, Germany) or by treating the plate with Enhance spray and exposing to X-ray films for 4 days at −80 °C.

Schiz. pombe random spore analysis

Plasmid transformation was performed using the lithium acetate procedure described in [23]. Transformants were grown on minimal medium containing 2 μM thiamin to suppress expression of the gene. Cells were then sporulated on solid EMM2 medium containing uracil (75 mg/l), but not histidine or leucine. Upon digestion of the ascal walls and remaining vegetative cells, 5000 spores were plated on solid EMM2 medium containing glutamic acid (5 g/l) as nitrogen source, adenine (10 mg/l), uracil (75 mg/l) and leucine (75 mg/l), but not histidine or thiamin. As a control, another 5000 spores were plated on the same medium containing 75 mg/l histidine. A limiting concentration of adenine in the medium allowed verification that growing cells are haploid, as these form pink and red colonies whereas diploid cells would appear white due to intragenic complementation of the *ade6-M210*/*ade6-M216* alleles.

PCR verification of the genotype of viable *Schiz. pombe* haploids

Primers specific for the *gpi1*$^+$::*his7*$^+$ locus were designed (U-His, 5′-TTGTTATGTTCCAGTAACAGTGAATTCCTG; D-gpi1, 5′-TGGATCCAAGAGACATCGGTTTGGAGTTGC). Whole-cell PCR was performed using the protocol given in [34]. In a second PCR reaction, the presence of the transformed mammalian *GPI1* gene was shown using primers U-Hs-*Nde*I and D-Hs-*Bam*HI (see above). In both PCRs, colonies from the parental wild-type strain were assayed as negative controls.

RESULTS

Cloning of human *GPI1*

A search of the EST database for sequences encoding peptides showing identity with *Sacch. cerevisiae* Gpi1p, and a subsequent search for larger clones with overlapping 3′ sequences, yielded several cDNA clones with inserts of up to 2.5 kb. To estimate the size of the full-length transcript, we performed Northern analysis of total RNA from HL-60 cells. A single weak band of 3 kb was obtained in two separate assays (results not shown). Cloning of the missing 5′ region was accomplished by using a RACE PCR-related technique (see the Materials and methods section). The full-length cDNA contains a 1743 bp ORF encoding 581 amino acids, as well as 50 bp upstream and 1100 bp downstream untranslated regions.

Identification of mouse *GPI1*

The cDNA sequence of *HsGPI1* was used to search the EST database again. A 3 kb mouse clone could be identified. It was not detectable in the initial database searches because it lacked a 3′ EST entry. Sequencing of this clone revealed 82 % identity with the *HsGPI1* coding region at the nucleic acid sequence level. The deduced protein sequence of 581 amino acids is 85 % identical to the human Gpi1 protein (Figure 1).

Protein sequence analysis

Human and mouse Gpi1 proteins have calculated molecular masses of 65.3 and 65.9 kDa respectively. CLUSTAL W dual sequence alignments [28] revealed 24 % and 19 % amino acid sequence identity with the *Sacch. cerevisiae* and *Schiz. pombe* proteins respectively for both sequences, whereas the yeast proteins are 29 % identical. However, due to a marked difference in size between the four proteins (*Schiz. pombe* Gpi1p comprises 517 amino acids, whereas *Sacch. cerevisiae* Gpi1p comprises 609 amino acids), these values do not correlate well with the actual degree of relationship. Therefore the guide tree file produced by CLUSTAL multiple sequence alignment was used to draw the phylogenetic tree shown in Figure 2. Intriguingly, mouse Gpi1p is somewhat more similar to the yeast proteins than human Gpi1p. Multiple sequence alignment demonstrates that the C-terminal half of the proteins is much better conserved than the N-terminal half (Figure 1). A potential tyrosine phosphorylation site is predicted by the PROSITE software package to occur in all four Gpi1 proteins (general consensus R/K-$X_{2,3}$-D/E-$X_{2,3}$-Y; consensus for Gpi1 proteins R-X-R-X-D-$X_{2,3}$-Y). This site is located on the third cytoplasmic loop of the protein (see below). Targeting signals such as organelle transit peptides, DNA binding sites or N-terminal secretory signals were not detected using standard predictive software.

Hydropathy plots performed according to Kyte and Doolittle [35] revealed multiple hydrophobic regions that could function as transmembrane segments (Figure 3). Regions predicted to be membrane-spanning with $P < 0.1$ by the Klein, Kanehisa and DeLisi algorithm [36] are indicated in the Figure. To predict Gpi1p membrane topology, we applied recently developed algorithms by Persson and Argos [31]. The results obtained were used to draw the predictive model in Figure 4. Intriguingly, the majority of amino acids are located on the cytoplasmic face of the endoplasmic reticulum. In contrast, most intraluminal loops are very small, serving as turns between transmembrane helices rather than building a significant domain. Also, cytoplasmic domains harbour most of the conserved residues, while structures in the endoplasmic reticulum lumen differ significantly between species, both in size and in amino acid composition.

Expression of mammalian *GPI1* in *Sacch. cerevisiae*

We constructed expression plasmids containing the coding region of either mouse or human *GPI1* directly behind the 343 bp upstream untranslated region from *ScGPI1* that was shown to contain sufficient promoter activity [16]. Additionally, a chimaeric

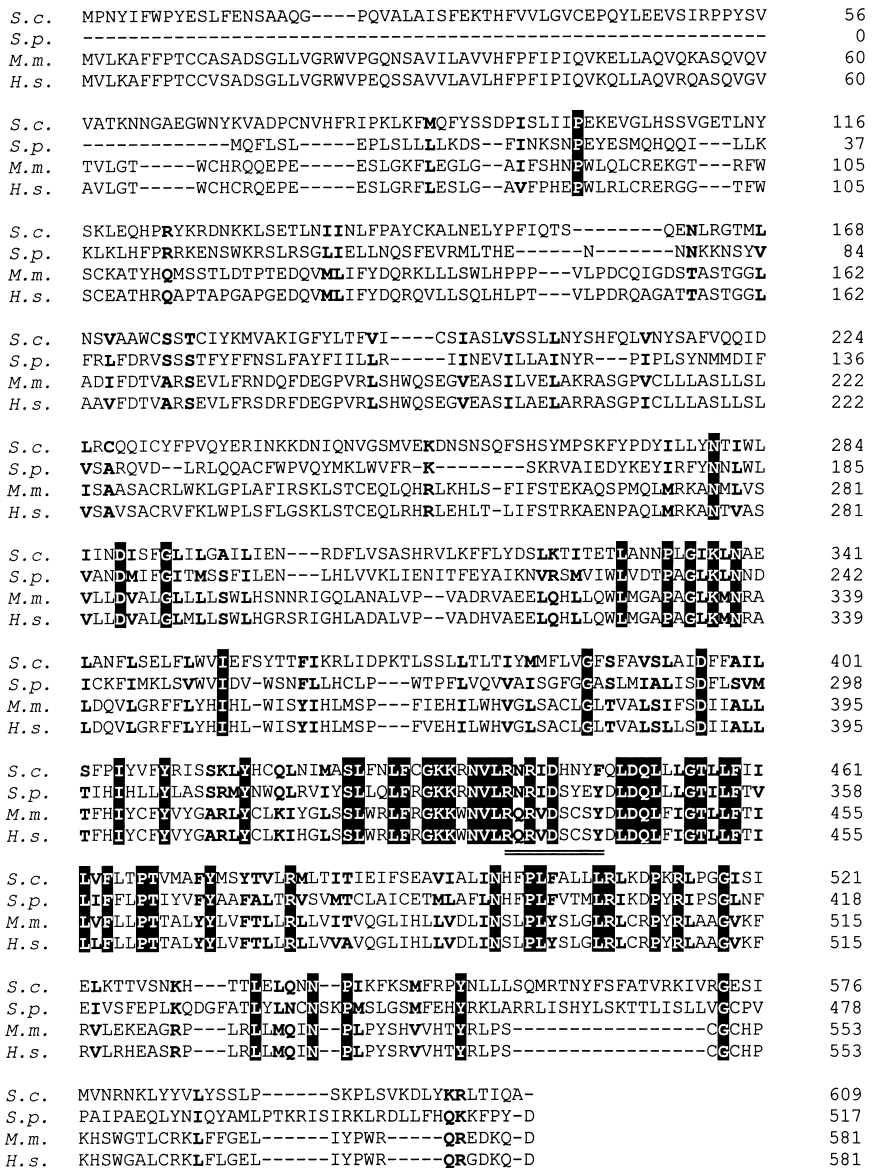

Figure 1 Identity between mammalian and yeast Gpi1 proteins is concentrated towards the C-terminus

CLUSTAL W multiple sequence alignment parameters were as follows: protein weight matrix, BLOSUM series; gap open penalty, 10 (default); gap extension penalty, 0.05 (default). Black boxes indicate amino acids identical in all proteins, and bold type without boxes indicates well conserved residues. A tyrosine phosphorylation site is predicted by PROSITE for all proteins [underlined; amino acids 439–446 in *Sacch. cerevisiae* (S.c.), 338–344 in *Schiz. pombe* (S.p) and 435–441 in the mammalian proteins (M.m, *Mus musculus*; H.s., *Homo sapiens*)]. All nucleotide and protein sequences are accessible at GenBank under AF030177 (human *GPI1*) and AF030178 (mouse *GPI1*).

ORF (termed *ScHsGPI1*) was constructed by replacing the well conserved C-terminus of ScGpi1p with that from HsGpi1p, yielding a protein 67% identical to ScGpi1p. All constructs were transformed into *Sacch. cerevisiae* Δ*gpi1* cells as both single- and multi-copy plasmids using CEN and 2μ origin of replication vectors respectively.

We first examined whether transformation with mammalian *GPI1* genes has an impact on the temperature-sensitivity of the *gpi1* knockout strain. As demonstrated in Figure 5, Δ*gpi1* cells transformed with a vector negative control grew at 25 °C, but not at 30 °C or 37 °C (sector 2 on each plate), whereas introduction of the wild-type *ScGPI1* gene on a single-copy plasmid completely restored the ability to grow at 30 °C and 37 °C (sector 1). Transformation of *HsGPI1* on a single-copy plasmid does not seem to have an effect on the temperature-sensitivity of the knockout cell line, since no growth was observed at 30 °C or 37 °C (Figure 5A, sector 3). However, Δ*gpi1* cells harbouring *HsGPI1* on a multi-copy plasmid were able to grow at 30 °C (Figure 5A, sector 4). Transformation of *MmGPI1* in a single-copy plasmid resulted in a few small colonies at 30 °C, whereas no growth was observed at 37 °C (Figure 5B, sector 3). In a multi-copy plasmid, *MmGPI1* allowed almost full restoration of growth at 30 °C and a few colonies at 37 °C (Figure 5B, sector 4). Results obtained upon transformation with the chimaeric *ScHsGPI1* gene were identical with those obtained with *MmGPI1* (results not shown).

To demonstrate further that the positive effect on growth at 30 °C and 37 °C is due specifically to restored GPI biosynthesis,

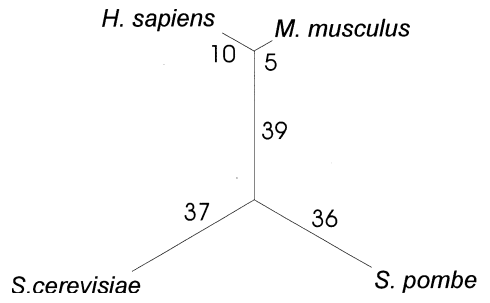

Figure 2 Phylogenetic relationships between mammalian and yeast Gpi1 proteins

The guide tree file calculated for the CLUSTAL alignment in Figure 1 was used to depict relationships between Gpi1 proteins from *Sacch. cerevisiae*, *Schiz. pombe*, *M. musculus* (mouse) and *H. sapiens* (human). Each number shown corresponds to the phylogenetic distance *d* multiplied by 100.

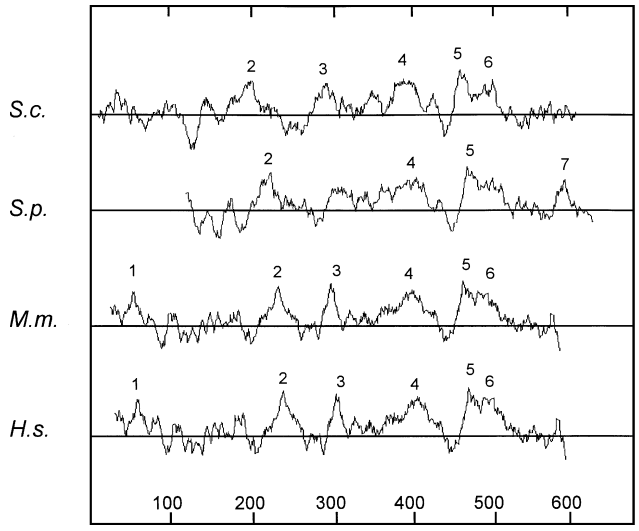

Figure 3 Mammalian and yeast Gpi1 proteins harbour multiple corresponding transmembrane segments

Hydropathy plots according to Kyte and Doolittle [35] were outlined truly to scale, but oriented to the highly conserved C-terminus to align corresponding segments. Small numbers on hydrophobic peaks indicate membrane-spanning regions predicted by the Klein, Kanehisa and DeLisi algorithm [36] with $P < 0.1$. The significance of peak 1, only present in mammalian Gpi1p, was not confirmed by using another predictive algorithm [31]. Therefore peak 2 corresponds to the first transmembrane domain in the model shown in Figure 4. Peak 3 corresponds to the second transmembrane segment, and peak 4 to the third and fourth transmembrane segments (these are most probably two distinct helices rather than one continuous one). Finally, peaks 5 and 6 correspond to the fifth and sixth transmembrane segments. *S.c.*, *Sacch. cerevisiae*; *S.p.*, *Schiz. pombe*; *M.m.*, *Mus musculus*; *H.s.*, *Homo sapiens*.

we prepared a mixed membrane fraction from our transformants and tested them for *in vitro* GlcNAc-PI synthetic activity. As shown in Figure 6, Δ*gpi1* membranes were unable to synthesize any [^{14}C]GlcNAc-PI (lane 2), but GlcNAc-PI synthetic activity was restored upon introduction of the wild-type *ScGPI1* gene on a single-copy plasmid (lane 1). Transformants harbouring *MmGPI1* on a multi-copy plasmid showed approx. 50% synthetic activity in comparison with the wild-type (lane 4), whereas the synthetic activity of membranes harbouring chimaeric *ScHsGPI1* did not differ from that of those with the wild-type

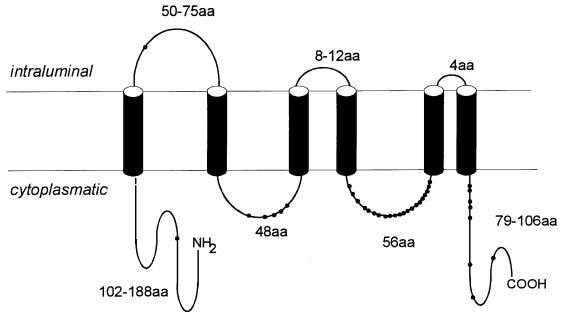

Figure 4 Membrane topology of Gpi1 proteins

The figure was drawn using data predicted by the Persson and Argos algorithm [31]. In brief, Gpi1 protein sequences from *Sacch. cerevisiae*, *Schiz. pombe*, *M. musculus* and *H. sapiens* were submitted simultaneously, sequences were aligned by the program and predictions were subsequently computed to fit the consensus. The results indicate that both termini are located cytoplasmically. The sizes of the first cytoplasmic and intraluminal domains, given as numbers of amino acids (aa) on the respective loops, differ between the four species. This is consistent with the shifting of peak 2 in Figure 3. Dots on the loops indicate completely conserved amino acids. These are almost exclusively located on cytoplasmic domains. The phosphotyrosine site indicated in Figure 1 is located on the third cytoplasmic domain.

gene (lane 5). However, using *HsGPI1* under the same conditions, only marginal GlcNAc-PI synthesis was detectable, despite five times longer fluorographic exposiure (results not shown).

To confirm the nature of the lipids produced in heterologously restored yeast membranes, these were subjected to chemical and enzymic analysis. As expected, GlcNAc-PI and GlcN-PI from membranes harbouring the mouse Gpi1 protein were completely sensitive to PI-specific phospholipase C (PI-PLC) and mild base hydrolysis (Figures 7A–7C). GlcN-PI was also susceptible to nitrous acid deamination (Figure 7D). When *in vitro* synthesis of GPI intermediates was performed in the presence of palmitoyl-CoA, GlcN-PI was inositol-acylated to form GlcN-(acylinositol)PI (Figure 7E). This intermediate was also sensitive to mild base hydrolysis and nitrous acid deamination, but was resistant to PI-PLC (Figures 7F–7H). Yeast membranes with a mammalian Gpi1 protein thus synthesize the same GPI precursors as are made in wild-type membranes.

Two further characteristics of the Δ*gpi1* mutation in *Sacch. cerevisiae* were tested: doubling time at 25 °C and morphological aberrations. Δ*gpi1* cells transformed with a vector control grew very slowly at 25 °C in minimal medium and had a doubling time of ~ 360 min. When transformed with the mammalian *GPI1* genes on multi-copy plasmids, they divided approximately every 240 min, similarly to transformants rescued with the *ScGPI1* wild-type gene. When shifted to 30 °C, Δ*gpi1* mutants show a characteristic morphology, with large, round, multiply budded cells when examined by phase-contrast microscopy. Both *HsGPI1* and *MmGPI1* were able to suppress this defect (results not shown).

Expression of mammalian *GPI1* in *Schiz. pombe*

In the fission yeast *Schiz. pombe*, *gpi1*$^+$ disruption is lethal. Therefore we used a heterozygous diploid strain harbouring one *gpi1*$^+$ allele that had been disrupted by the *his7*$^+$ gene as a selectable auxotrophic marker (*gpi1*$^+$::*his7*$^+$). After transformation with mammalian *GPI1* genes or positive and negative controls, cells were starved to induce meiosis and sporulation. Equal numbers of spores were plated on medium selective for the disrupted *gpi1*$^+$::*his7*$^+$ allele, such that cells would only grow if mammalian *GPI1* genes were able to substitute for the wild-type

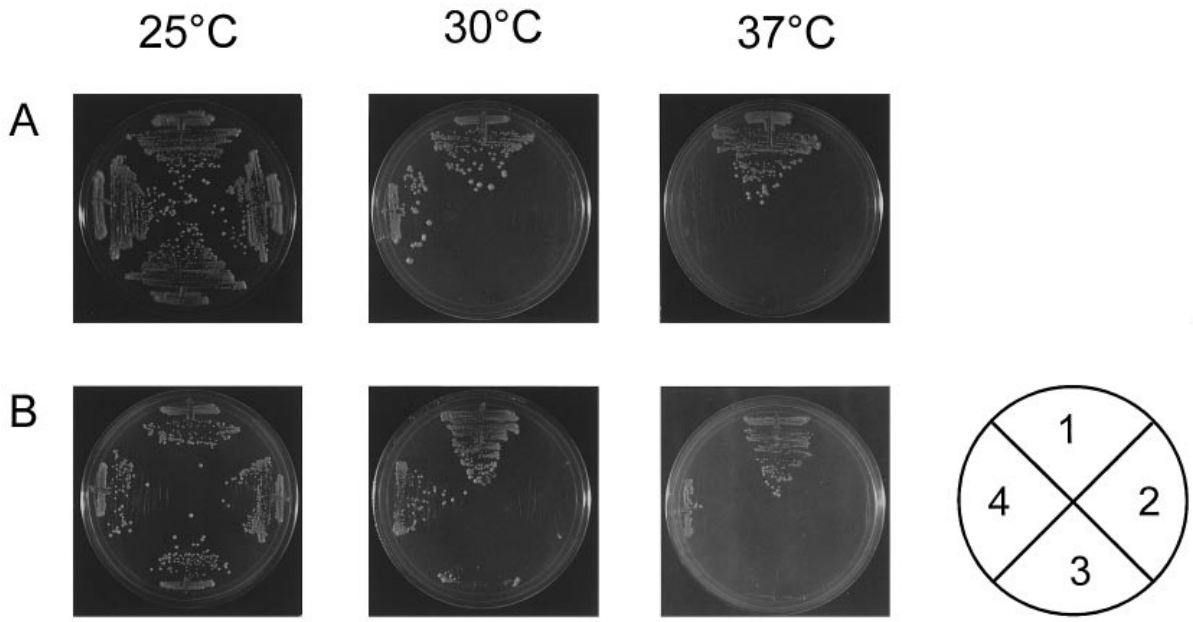

Figure 5 Mammalian *GPI1* genes partially complement the temperature-sensitivity of the *Sacch. cerevisiae* Δ*gpi1* mutation

Mammalian *GPI1* genes were expressed in yeast Δ*gpi1* cells to provide evidence for functional identity between the yeast and mammalian gene products. Key: sector 1, wild-type *ScGPI1* gene; sector 2, vector control; sector 3, mammalian gene behind the native yeast *GPI1* promoter in a single-copy plasmid (CEN); sector 4, mammalian gene behind the yeast *GPI1* promoter in a multi-copy plasmid (2μ). (**A**) Human *GPI1* rescues Δ*gpi1* at 30 °C when introduced on a multi-copy plasmid. (**B**) Mouse *GPI1* almost completely restores growth at 30 °C and rescues a few colonies at 37 °C when transformed into Δ*gpi1* with a multi-copy plasmid.

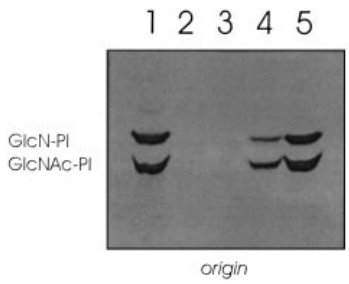

Figure 6 Mammalian *GPI1* genes restore *in vitro* GlcNAc transferase activity

The *Sacch. cerevisiae* Δ*gpi1* strain was transformed with: lane 1, *ScGPI1* wild-type gene; lane 2, vector control; lane 3, *HsGPI1*; lane 4, *MmGPI1*; lane 5, *ScHsGPI1* (chimaeric ORF exchanging only the well conserved C-terminal part of Gpi1p). Washed yeast membranes were incubated with UDP-[^{14}C]GlcNAc, and radiolabelled lipids were extracted and separated by TLC. The wild-type, mouse and chimaeric proteins restore the activity of the GlcNAc transferase complex. Formation of deacetylated GlcN-PI, the second intermediate in GPI biosynthesis, is restored as well, because the substrate for this reaction, GlcNAc-PI, becomes available.

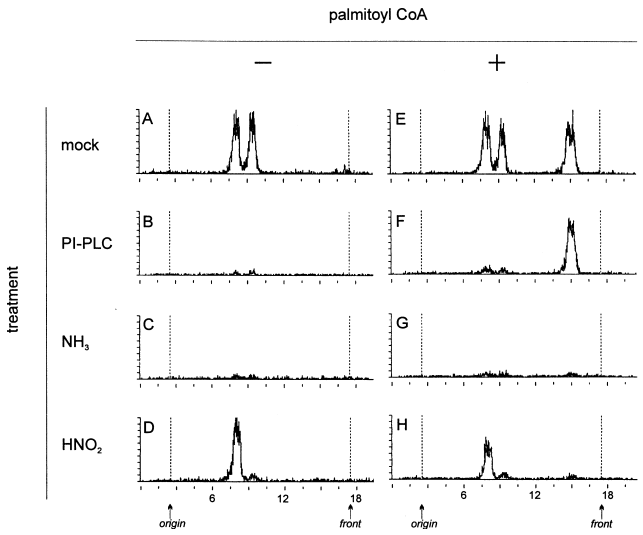

Figure 7 Chemical and enzymic analysis of the GPI intermediates produced in the presence of mouse Gpi1p

Membranes from the *Sacch. cerevisiae* Δ*gpi1* strain transformed with *MmGPI1* on a multi-copy plasmid were incubated with UDP-[^{14}C]GlcNAc alone (**A**–**D**) or UDP-[^{14}C]GlcNAc plus palmitoyl-CoA (**E**–**H**). Radiolabelled lipids were treated as indicated and analysed by TLC. Mock-treated membranes (**A** and **E**) showed the formation of GlcNAc-PI, GlcN-PI and, if palmitoyl-CoA was added, GlcN-(acylinositol)PI (in the order of their appearance from origin to front). GPI-specific PI-PLC hydrolyses GlcNAc-PI and GlcN-PI, but not GlcNAc-(acylinositol)PI (**B** and **F**). All intermediates are completely susceptible to treatment with methanolic NH_3 (mild base; **C** and **G**). Nitrous acid deamination confirms the presence of a free amine group in GlcN-PI and GlcN-(acylinositol)PI, but not in GlcNAc-PI (**D** and **H**).

gpi1$^+$ gene. Figure 8(A) shows colony formation after 7 days of incubation at 30 °C, and demonstrates that both mouse and human *GPI1* genes rescued haploid cells, although the number of growing colonies was significantly lower than that obtained with the wild-type positive control. Cells did not reveal any morphological disorders when examined by phase-contrast microscopy. To verify that the viable colonies were indeed *gpi1*$^+$::*his7*$^+$ disrupted haploids surviving only because of the presence of the

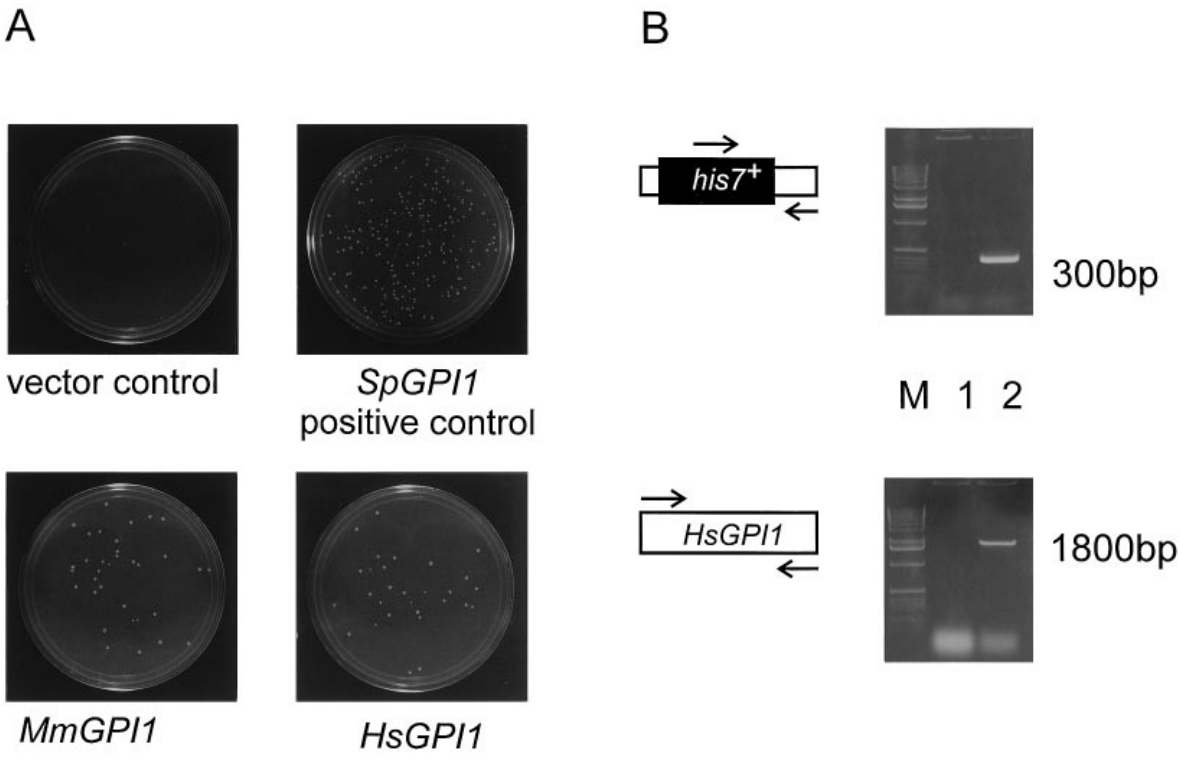

Figure 8 Mammalian *GPI1* genes complement the lethal *Schiz. pombe gpi1*$^+$ mutation

(**A**) Human and mouse *GPI1* genes, as well as positive and negative controls, were transformed into *gpi1*$^+$/*gpi1*$^+$::*his7*$^+$ heterozygous *Schiz. pombe* diploids. Upon meiosis and sporulation, spores were allowed to germinate under selection for the lethal *gpi1*$^+$::*his7*$^+$ allele, allowing survival of only those cells with a functional *gpi1*$^+$ equivalent on a plasmid. (**B**) Whole-cell PCR with primers specific for the *gpi1*$^+$::*his7*$^+$ locus and the transformed human or mouse gene. Lane 1, colony from the parental wild-type strain as a negative control; lane 2, haploid *gpi1*$^+$::*his7*$^+$ colony containing *HsGPI1*; lane M contains size markers.

mammalian *GPI1* gene, colonies were analysed by whole-cell PCR with primers specific for the *gpi1*$^+$::*his7*$^+$ allele and the mammalian *GPI1* gene on the plasmid (Figure 8B). All haploid colonies were found to have the expected genotype. In contrast, not one out of 15 randomly chosen colonies that grew on plates without selection for the *gpi1*$^+$::*his7*$^+$ disruption revealed that genotype.

DISCUSSION

Our results confirm the existence of a postulated fourth participant in the mammalian GlcNAc-PI synthetic machinery. The newly cloned human and mouse cDNAs specifically rescue yeast Δ*gpi1* mutants and therefore are indeed involved in the first step of GPI biosynthesis.

In *Sacch. cerevisiae*, we observed a dose- and temperature-dependent effect of mammalian *GPI1* genes on the Δ*gpi1* phenotype: whereas expression of single-copy genes had little or no effect, moderate overexpression of the heterologous genes in multi-copy plasmids was able to suppress all characteristics of the Δ*gpi1* mutation examined. In general, effects at 30 °C were more prominent than at 37 °C. This observation strongly suggests that Gpi1p, in contrast with Gpi2 and Gpi3, is important in stabilizing a GlcNAc-PI synthetic protein complex in the endoplasmic reticulum. At temperatures of 25 °C and 30 °C, mammalian Gpi1 proteins are able to participate in the complex and almost completely suppress the Δ*gpi1* phenotype. At 37 °C, functioning of the GlcNAc synthetic complex is seriously impaired when a heterologous Gpi1 replaces the native protein. This is in contrast with the general principle that enzymes gain in activity at increasing temperatures, and indicates a specific function of Gpi1p as an integrating stabilizer of the enzymic complex. Further support for this hypothesis comes from our *in vitro* experiments. Viable Δ*gpi1* cells are able to produce GPI anchors at 25 °C, as demonstrated by the *in vivo* incorporation of [^{3}H]inositol into proteins [9]. In contrast, isolated and purified membranes from these cells do not show any synthetic activity *in vitro*. These data suggest that the incomplete GlcNAc transferase complex without Gpi1p does not endure the rough process of membrane preparation, including repeated homogenization and centrifugation. Mammalian Gpi1 proteins partially restore the stability of the complex and allow detection of *in vitro* synthetic activity again.

Lipids synthesized in the presence of mammalian Gpi1p are not distinguishable from lipids made in wild-type *Sacch. cerevisiae* membranes. Also, biosynthetic steps subsequent to GlcNAc-PI formation are not affected, as shown for deacetylation and inositol acylation, the second and third steps of the pathway. Gpi1p is unlikely to be additionally involved in catalysis or regulation of one of these reactions, since Δ*gpi1* membranes are capable of producing GlcN-PI and GlcN-(acylinositol)PI from GlcNAc-PI (D. Drapp and P. Orlean, unpublished work).

In all *Sacch. cerevisiae* experiments, and most dramatically in the *in vitro* assay, mouse *GPI1* seems to be more efficient than human *GPI1*. This is consistent with the observation that the phylogenetic relationship between the yeast and mouse proteins is somewhat closer than that between the yeast and human proteins (Figure 2). Moreover, these results indicate that the

protein complex containing a heterologous Gpi1p is far from being comparable with the native enzymic complex, because small differences in the sequence of the transformed gene or in the strength of expression can dramatically diminish the observed effects. Therefore mammalian *GPI1* genes in *Sacch. cerevisiae* mutants provide a unique opportunity to look at structure/function relationships and partial defects in GPI biosynthesis. Also, the partially restored Δ*gpi1* strains can be used as a tool to search for further genes involved in GPI biosynthesis.

In *Schiz. pombe*, we demonstrated that both human and murine *GPI1* genes can rescue haploid cells harbouring the lethal *gpi1*$^+$::*his7*$^+$ mutation. Random spore analysis was used in this experiment, since only a portion of *Schiz. pombe* cells form colonies after tetrad dissection, even if wild-type strains are used. The number of *gpi1*$^+$::*his7*$^+$ haploids that could be rescued by the mammalian genes was significantly lower than when the wild-type *Schiz. pombe gpi*1$^+$ gene was used. In addition, the native gene had an advantage when selection for *gpi1*$^+$::*his7*$^+$ was removed. However, after successful spore germination, haploids harbouring the mammalian *GPI1* gene did not show any disorders in growth or morphogenesis.

The fact that mammalian *GPI1* genes can replace the respective yeast genes does not only provide evidence for their identity, but is an important result in itself. Considering the notion that homology is indicative of functional similarity, our data clearly demonstrate that mammalian and yeast Gpi1 proteins are not only structurally similar but also functionally equivalent. This indicates that the molecular mechanisms that underlie this step in GPI biosynthesis have been extremely well conserved throughout evolution. In contrast, marked differences in downstream steps of yeast/mammalian and protozoal GPI pathways have been elucidated [37–39]. These biochemical steps might serve as targets for anti-microbial pharmacotherapy in the future.

Further work will focus on the role of *GPI1* in mammalian cells. In the absence of a cell line deficient in *GPI1*, it remains to be demonstrated whether Gpi1p is essential for GPI biosynthesis in mammals. Following the conclusion that yeast Gpi1p most probably acts as a stabilizing factor, preserving the integrity of the enzymic complex (especially at higher temperatures), it is possible that Gpi1p may not be an essential component of the mammalian GlcNAc transferase complex at all, or it may only be required under certain conditions. However, certain regions within the Gpi1p homologues are strictly conserved and therefore are likely to carry essential functions within the complex. One of these is a putative tyrosine phosphorylation site. This structure could be involved in the regulation of GPI biosynthesis, which one would expect to take place in its first step. Indeed, GPI biosynthesis was previously shown to be very rapidly stimulated during T-cell activation, but almost nothing is known about the underlying molecular mechanisms. Since Gpi1p is likely to contain multiple transmembrane segments, it could also play a role in early interactions of the enzymic complex with fatty acids of its substrate, PI. An understanding of these details of the unexpectedly complex enzymology of GlcNAc transfer in GPI biosynthesis could further help to explain the pathophysiology of PNH.

This work was supported by Deutsche Forschungsgemeinschaft grant DFG Schu 713/2-3 (to J.S.), by National Institutes of Health grant GM46220 (to P.O.), and by the Volkswagen Stiftung. We thank the Studienstiftung des deutschen Volkes for generously supporting A.T.'s stay in Urbana-Champaign. We are indebted to Eric C. Böttger and Kerstin Techner (Hannover Medical School, Dept. of Medical Microbiology) for sequencing many cDNA clones. For help with yeast techniques we acknowledge Steven Grimme, Zlatka Kostova and Eric Robinson. We further thank Ingo Bastisch, Iska Janssen-Graalfs, Carsten Schiller and J. Engelbert Gessner for many helpful discussions and contributions to this work.

REFERENCES

1 Ferguson, M. A. and Williams, A. F. (1988) Annu. Rev. Biochem. **57**, 285–320
2 Ravetch, J. V. (1994) Cell **78**, 553–560
3 Kinoshita, T., Inoue, N. and Takeda, J. (1995) Adv. Immunol. **60**, 57–103
4 Hirose, S., Ravi, L., Hazra, S. V. and Medof, M. E. (1991) Proc. Natl. Acad. Sci. U.S.A. **88**, 3762–3766
5 Armstrong, C., Schubert, J., Ueda, E., Knez, J. J., Gelperin, D., Hirose, S., Silber, R., Hollan, S., Schmidt, R. E. and Medof, M. E. (1992) J. Biol. Chem. **267**, 25347–25351
6 Schubert, J., Schmidt, R. E. and Medof, M. E. (1993) J. Biol. Chem. **268**, 6281–6287
7 Schubert, J., Uciechowski, P., Zielinska Skowronek, M., Tietjen, C., Leo, R. and Schmidt, R. E. (1992) J. Immunol. **148**, 3814–3819
8 McConville, M. J. and Ferguson, M. A. (1993) Biochem. J. **294**, 305–324
9 Leidich, S. D., Drapp, D. A. and Orlean, P. (1994) J. Biol. Chem. **269**, 10193–10196
10 Colussi, P. A. and Orlean, P. (1997) Yeast **13**, 139–150
11 Englund, P. T. (1993) Annu. Rev. Biochem. **62**, 121–138
12 Stevens, V. L. and Raetz, C. R. (1991) J. Biol. Chem. **266**, 10039–10042
13 Miyata, T., Takeda, J., Iida, Y., Yamada, N., Inoue, N., Takahashi, M., Maeda, K., Kitani, T. and Kinoshita, T. (1993) Science **259**, 1318–1320
14 Inoue, N., Watanabe, R., Takeda, J. and Kinoshita, T. (1996) Biochem. Biophys. Res. Commun. **226**, 193–199
15 Kamitani, T., Chang, H. M., Rollins, C., Waneck, G. L. and Yeh, E. T. (1993) J. Biol. Chem. **268**, 20733–20736
16 Leidich, S. D. and Orlean, P. (1996) J. Biol. Chem. **271**, 27829–27837
17 Leidich, S. D., Kostova, Z., Latek, R. R., Costello, L. C., Drapp, D. A., Gray, W., Fassler, J. S. and Orlean, P. (1995) J. Biol. Chem. **270**, 13029–13035
18 Fassler, J. S., Gray, W., Lee, J. P., Yu, G. Y. and Gingerich, G. (1991) Mol. Gen. Genet. **230**, 310–320
19 Vossen, J. H., Ram, A. F. and Klis, F. M. (1995) Biochim. Biophys. Acta **1243**, 549–551
20 Schönbächler, M., Horvath, A., Fassler, J. and Riezman, H. (1995) EMBO J. **14**, 1637–1645
21 Zieler, H. A., Walberg, M. and Berg, P. (1995) Mol. Cell. Biol. **15**, 3227–3237
22 Rose, M. D., Winston, F. and Hieter, P. (1990) Methods in Yeast Genetics: A Laboratory Course Manual, Cold Spring Harbor Laboratory Press, Cold Spring Harbor, NY
23 Alfa, C., Fantes, P., Hyams, J., McLeod, M. and Warbrick, E. (1993) Experiments with the Fission Yeast: A Laboratory Course Manual, Cold Spring Harbor Laboratory Press, Cold Spring Harbor, NY
24 Boguski, M. S., Lowe, T. M. and Tolstoshev, C. M. (1993) Nature Genet. **4**, 332–333
25 Altschul, S. F., Gish, W., Miller, W., Myers, E. W. and Lipman, D. J. (1990) J. Mol. Biol. **215**, 403–410
26 Lennon, G., Auffray, C., Polymeropoulos, M. and Soares, M. B. (1996) Genomics **33**, 151–152
27 Marck, C. (1988) Nucleic Acids Res. **16**, 1829–1836
28 Thompson, J. D., Higgins, D. G. and Gibson, T. J. (1994) Nucleic Acids Res. **22**, 4673–4680
29 Schuler, G. D., Altschul, S. F. and Lipman, D. J. (1991) Proteins **9**, 180–190
30 Fuchs, R. (1991) Comput. Appl. Biosci. **7**, 105–106
31 Persson, B. and Argos, P. (1997) J. Protein Chem. **16**, 453–457
32 Maundrell, K. (1993) Gene **123**, 127–130
33 Costello, L. C. and Orlean, P. (1992) J. Biol. Chem. **267**, 8599–8603
34 Jesnowski, R., Naehring, J. and Wolf, K. (1995) Curr. Genet. **27**, 318–319
35 Kyte, J. and Doolittle, R. F. (1982) J. Mol. Biol. **157**, 105–132
36 Klein, P., Kanehisa, M. and DeLisi, C. (1985) Biochim. Biophys. Acta **815**, 468–476
37 Güther, M. L. and Ferguson, M. A. (1995) EMBO J. **14**, 3080–3093
38 Sütterlin, C., Horvath, A., Gerold, P., Schwarz, R. T., Wang, Y., Dreyfuss, M. and Riezman, H. (1997) EMBO J. **16**, 6374–6383
39 Smith, T. K., Sharma, D. K., Crossman, A., Dix, A., Brimacombe, J. S. and Ferguson, M. A. (1997) EMBO J. **16**, 6667–6675

Received 12 February 1998/17 June 1998; accepted 6 July 1998